Alignment of Small Organic Solutes in a Nematic Solvent: The Effect of Electrostatic Interactions.

A. Pizzirusso, M. B. Di Cicco, G. Tiberio, L. Muccioli, R. Berardi and C. Zannoni[*]

Dipartimento di Chimica Fisica e Inorganica, and INSTM,

Viale Risorgimento 4, 40136 Bologna, Italy

E-mail: claudio.zannoni@unibo.it

Abstract

The origin of the alignment with respect to the director observed for solutes in a nematic host remains unclear and various mechanisms ranging from steric repulsions to dispersive or electrostatic interactions have been invoked. Here we present atomistic molecular dynamics (MD) computer simulations of rigid solutes of small dimensions dissolved in a nematic liquid crystal solvent, 4-n-pentyl,4$'$cyanobiphenyl (5CB), that aim to quantitatively predict the orientational order. We have validated the results comparing the dipolar couplings obtained by atomistic simulation with their experimental NMR counterparts. To help assessing the separate effect of the various types of anisotropic interactions on the orientational order of solutes, we have modelled solute molecules both with their partial atomic charges present or absent (switching them to zero) finding that, at least for the cases studied, the alignment mechanism is largely dominated by steric and van der Waals dispersive forces rather than Coulomb ones. We have compared the anisotropic aligning potential with the predictions of the Maier-Saupe and surface tensor models and discussed their performance.

[*]To whom correspondence should be addressed

Introduction

Nuclear Magnetic Resonance (NMR) spectroscopy is widely used for investigating both long-range orientational order in liquid crystals and the geometrical properties of solutes dissolved in these mesophases. The orientational order of the solvent in fact allows the measurement of structure-sensitive anisotropic properties[1–5] such as nuclear dipolar couplings, that would instead average to zero in isotropic liquids. Similar concepts have been employed with great success for the structural investigation of proteins in weakly aligning media.[6] The analysis of the NMR spectra for small molecules dissolved in liquid crystals has resulted in a large body of information about molecular properties, notably molecular conformations and orientations, derived from direct dipolar coupling, quadrupolar coupling and indirect coupling tensors.[1,3,5,7–9] As long as the number of coupled spins in the solute molecules is relatively small, well resolved NMR spectra can usually be observed. In the most important case of proton NMR, this well resolved spectrum is superimposed to a broad background due to the unresolved spectrum of the nematic solvent.[10]

Over the years various theoretical models have been proposed for rationalizing the experimental observations, but none of these has prevailed and there are still unanswered questions. A large number of studies[1,3,5,7,11–19] have tried to relate specific molecular features (structure, electric multipoles, shape, surface, polarizability) to the orientational order of the host liquid crystal (LC). Unfortunately, an unavoidable problem in analysing real experimental data with the aim of assessing the relative importance of the various types of interactions, is that all the contributions to the intermolecular energy are superimposed and cannot be easily separated. To get some hints, homologous series of molecules which differ only for a certain chemical substitution that selectively alters a property, can be used. For instance in a family of substituted benzenes, F, Br and Cl atoms could be systematically inserted at the same position to examine the effect of different electronegativity or polarizability.

Yet another strategy that has been pursued, is to use various nematic solvents while keeping the same solute. In particular Burnell, de Lange and coworkers have put forward the use of mixtures of nematics with opposite sign of the dielectric anisotropy so as to compensate electric field gradient

effects.[1] They argued that it is possible to choose solvent combinations that in certain physical conditions, like composition or temperature, cancel out field gradient interactions (e.g. quadrupolar[20]), thus leaving steric forces (molecular shapes) as the dominant contribution. They calibrated these mixtures that are known as "magic mixtures" using small apolar solutes as described in.[1] In this context, the great advantage of simulations is the ability of selectively varying or even switching-off specific intermolecular contributions of the solute or the solvent without changing the chemical nature of the system.[15,21] In the past Monte Carlo simulations on coarse grained models based, e.g. on a Gay Berne representation of solutes and nematic solvents has been used[11,13] with the aim of looking at trends arising from one or multiple electric quadrupoles embedded in the Gay Berne ellipsoids. Recent advances in atomistic simulations of liquid crystals demonstrated the predictive capability of the technique[22–27] and suggested that more specific studies addressing the direct comparison with NMR experiments are possible. For istance, in[22] we have shown that the transition temperatures, densities, order parameters and NMR observables can be reproduced for the important series of n-cyanobiphenyls. It is important to assess if these advances in simulations can be applied to solutes at relatively low (a few %) concentration in nematics, where the statistics on solute properties such as dipolar couplings is inevitably much more problematic. This would, however, be quite important also in view of the recent developments in NMR data analysis [1,28,29] that allow for fairly automatic computerized method in the determination of dipolar couplings from spectral data. Then we here show the application of the atomistic Molecular Dynamics (MD) technique to investigate the order of rigid solutes in the nematic 5CB and the importance of their charge distribution on alignment. At the same time we assess the effect of solutes on the order of the nematic solvent. Thus, our study has the double intent of checking if the atomistic intermolecular potentials and the currently amenable sample sizes in MD simulations are capable of reproducing the experimental NMR observations, and at the same time of determining the specific aligning mechanism of the solute-solvent interactions. In addition we compare the alignment energy obtained by MD simulation with that expected from the approximate Maier-Saupe[30] and surface tensor[31] model theories.

3

Simulation details

We wish to make contact and compare our results with ^{1}H NMR experiments on small rigid solutes dissolved in nematics. These typically employ rod-like or disc-like solutes in concentrations of the order of 5% in weight on weight.[3] Since the orientational order of solutes in liquid crystals is widely influenced by their specific interactions with solvent, as well as by concentration, temperature and solvent purity, a standard reference molecule is often added to the solution to compare the results from different experiments at the same order for the reference solute. To mimic these experimental conditions, in our study the samples are composed of 2000 molecules, of which 1904 molecules of the solvent 4-n-pentyl,4$'$cyanobiphenyl (5CB), 16 molecules of 1,3,5-trichlorobenzene (TCB), as an internal standard, and 80 molecules of solute giving a mole fraction $x = 0.04$. These sample sizes are quite large for current atomistic simulations, but they are essential. Indeed in a preliminary set of simulations we have employed relatively small size samples with 238 molecules of solvent, 10 of solute and 2 of standard molecules but these simulations showed rms errors with magnitude $\geq 100\%$, quite unacceptable. Here we have studied the following solutes: benzene (BEN), 1,3,5-tribromobenzene (TBB) (disc-like), acetylene (ACE), propyne (PRO) and acetonitrile (ACN) (rod-like) (Figure 1). All of these have at least a C_3 symmetry axis and thus have effectively uniaxial symmetry as far as second rank NMR observables are concerned.[32] The solutes, including the standard, have been described with full atomistic details, the atomic charges[33] being computed at the minimum energy geometry, using the B3LYP density functional and the $6 - 31G^{**}$ basis set.[34] The 5CB solvent molecules have instead been described at united atoms (UA) level of detail, where CH, CH_2 and CH_3 groups are considered as spherical interaction sites, using a force field successfully tuned to reproduce its experimental nematic-isotropic transition temperature (T_{NI}).[22]

In order to assess the role of charges we have performed two series of simulations. First of all we have considered the complete force field and compared the MD simulation results with experimental NMR data; we have labelled these results as "standard solutes" or "q". After that, we have repeated the simulations "chargeless solutes" or "0" for not considering the electrostatic contribu-

tions to the intermolecular solute-solvent and solute-solute interactions. In the simulations this can be easily accomplished setting the atomic charges of the solute to zero. The differences between these results can be used to test the importance of electrostatic versus steric interactions. Experimentally a solvent that cannot establish such electrostatic interactions is defined as "magic".[1] So, in a way, in our simulations we have transformed our normal solutes in "magic solutes".

As we have already discussed in,[22] the equilibration time for realistic simulations should be longer then typical reorientation times of the molecules in the system; i. e. $10 - 20$ ns for 5CB solutions. This implies that repeating a full simulation from scratch for a sample of 2000 molecules for every solute can be very demanding (and wasteful). We have thus decided to start each simulation inserting the solute molecules in a preliminary equilibrated 5CB sample and re-equilibrating from there. Inserting a particle in a dense system is notoriously problematic, because of the high chance of overlaps and harsh repulsions. We have chosen as a convenient strategy to replace a solvent molecule with the solute to be inserted, scaled down in size if needed. In pratice we select inside the LC sample the solvent molecules to remove that present similar occupation of space of the solute to insert. For this purpose we have implemented the substitution comparing the inertia tensor of the solute to be inserted and of each of the solvent molecules inside an equilibrated configuration. If scaling down was performed the original solute size has been reestablished in the equilibration.

We have ran MD-NPT simulations using NAMD[35] at the following thermodynamic conditions: $P = 1$ atm, $T = 285$ K, 290 K, 295 K, 300 K and 305 K, using periodic boundary conditions. To maintain constant temperature and pressure we have used Berendsen's thermostat and barostat.[36] The solutes interactions have been calculated with the AMBER-OPLS force field.[37,38] The long range interactions have been computed via the particle mesh Ewald method[39] with a grid spacing of 1.2 Å, while the van der Waals interactions have been calculated within a cutoff of 12 Å. NAMD has the advantage of allowing different time steps for the dynamics equations consisting to different motions and here we adopted time step 1 fs for bonded interactions, 4 fs and 8 fs respectively for the van der Waals and electrostatic terms, and saved the trajectories every 10 ps for further analysis.

The typical MD simulation time for each solution was 40 ns, a time long enough to exceed, for these low molecular mass solutes, their typical reorientational relaxation time (see e. g.[7]) and to give a sufficient confidence that equilibration was achieved. Finally, to improve the comparison with some experimental data, we have also run a 60 ns-long MD simulation of pure 5CB, using a sample of $N = 2000$ molecules at equilibrating it at $P = 1$ atm and $T = 300$ K.

Orientational order

The order parameter $\langle P_2 \rangle$, that represents the second moment of the single molecule orientational distribution $\mathscr{P}(\cos \beta)$, is commonly used to characterise the average degree of alignment of a molecular axis $\mathbf{u}$, with respect to the preferred direction $\mathbf{n}$ of a liquid crystal host (aka the mesophase director):

$$\langle P_2 \rangle = \left\langle \frac{3}{2} \cos^2 \beta - \frac{1}{2} \right\rangle \equiv \left\langle \frac{3}{2} (\mathbf{u} \cdot \mathbf{n})^2 - \frac{1}{2} \right\rangle \ , \tag{1}$$

where β is the angle between the unit vectors $\mathbf{n}$ and $\mathbf{u}$. In particular we have computed the order parameters for the 5CB solvent $\langle P_2 \rangle_{\mathrm{LC}}$ and the solutes $\langle P_2 \rangle_{\mathrm{S}}$. For determining $\langle P_2 \rangle_{\mathrm{LC}}$ from an MD trajectory we used the standard algorithm relying on the diagonalisation of an ordering matrix.[32] This allows identifying the instantaneous director $\mathbf{n}$ for the configuration at time t, which can fluctuate when no external field is applied, and to compute the angles β_i between the phase director and the axis of each solute (or solvent) molecule. We have chosen the instantaneous reference molecular direction as the eigenvector of the inertia moment with lowest eigenvalue for the prolate molecules (acetylene, propyne and acetonitrile and 5CB itself), and that with the highest eigenvalue for the oblate ones (benzene, trichlorobenzene and tribromobenzene). For our rigid solutes this corresponds to the highest symmetry axis, while for a flexible molecule as 5CB this represents a convenient general method.

While the order parameters of a large number of solutes dissolved in nematic solvents have been studied by NMR[1,3,5] less attention has been given instead to the effect that the solutes have on the

orientational order of the nematic solvent itself,[40,41] due in part to the difficulty of disentagling and interpreting its many-lines NMR spectra. Using molecular dynamics simulations we are, however, in a unique position to determine also these solute-induced effects on 5CB alignment that we report in Figure 3 and in Table 1. We see that, as expected, the general outcome is that of lowering the solvent $\langle P_2 \rangle_{LC}$ and of shifting the nematic-isotropic transition to temperatures lower than 305 K, while the simulated value for pure 5CB is 310 K[22] and the experimental one is 308.2 K.[42] The quantitative effect on the T_{NI} seems to be comparable for all rod-like and disc-like solutes.

Among solutes endowed with their atomic charges, the lowering of the solvent order $\langle P_2 \rangle_{LC}$ obtained by MD seems to be more pronounced for the disc-like molecules (BEN and TBB), with elongated solutes like PRO and ACN perturbing the LC order less than bulkier ones. For the chargeless molecules, these effects seem to be less well defined and, within our statistical error (roughly estimated to $\sim 10\%$) all solutes give comparable results.

Close to the T_{NI}, propyne and acetylene affect the order more than the same solutes modelled without partial charges. In all these simulations, we noticed that the order parameter of 1,3,5-trichlorobenzene follows linearly the order of the solvent (Figure 2), hence its use as a standard is supported also by computer simulations results. Regarding the ordering properties of the solutes, we recall that the sign of the order parameter $\langle P_2 \rangle_S$ indicates the average orientation of their principal molecular axis with respect to the nematic director: positive for rod-like solutes and negative for disc-like solutes (see Figure 4 and Table 2). In all cases the calculated sign agrees with experiment. When excluding solute-solvent electrostatic interactions in the MD simulations we observe a general reduction of the solute order parameter in the nematic phase, while its sign is always conserved. Concluding the discussion about the solute alignment and also to better estimate the statistical errors in our simulations, it is worth mentioning that the quality of the prediction of the alignment is also measured by the ability of the simulations to obtain order parameters close to zero in the isotropic phase. This is not obvious as $\langle P_2 \rangle_{LC}$ are non negative by definition since they are obtained as the largest eigenvalue of the traceless ordering matrix.[22] $\langle P_2 \rangle_S$ is referred to the solvent director and thus can be positive or negative, but will become strictly zero only for

7

the number of particles N going to infinity. The values at 305 K reported in Table 2, where we consider the solvent to be isotropic, demonstrates that for our simulations any value of the solute order parameter is 0.05, which also corresponds to the standard deviation of our measurements, and should then be considered as isotropic.

Most of the published experimental data[3,5] are difficult to compare with ours, as they refer to nematic solvents different from 5CB and, moreover, measurements were often performed at only one temperature. Here, we have compared our results at 295 K with those available for solutes in 5CB[43] at 294 K (Table 3). We notice that they are generally in quantitative agreement, in particular for 1,3,5-tribromobenzene, acetylene and propyne, while for benzene the deviations are more significant but still within the confidence intervals. A further comparison is possible for the ordering of the solvent. In fact, deuterium quadrupolar splittings have been measured for deuterated 5CB pentyl hydrogens (labeled α-ω starting from the methylene group bonded to the phenyl and ending with the methyl group), the contribution arising from both for the pure compound[44] and in presence of some of the solutes.[43] Neglecting as usual the biaxiality of the nuclear quadrupole, we computed these observables as:

$$\Delta \nu_D = \frac{3}{2} q_{zz} \langle P_2 \rangle^{C-H} \tag{2}$$

where q_{zz} is the z component of the deuterium quadrupolar coupling tensor, here assumed equal to 160 kHZ,[45] and $\langle P_2 \rangle^{C-H}$ is the average order parameter of the deuterium-carbon bond (corresponding to the z axis of the tensor). Being the hydrogens implicit in our description of the 5CB molecules, we calculated their position and the direction of the $C-H$ bond on a geometrical basis,[22] and given the positive diamagnetic anisotropy of 5CB, we assumed the magnetic field of the NMR experiment parallel to the phase director. The simulations results, compared with experimental data, are shown in Table 4. An advantage of simulations with respect to the experiments is that they allow measuring also the sign of the splitting, which is always negative for the alkyl chain hydrogens. Commenting the values, it can be noticed that, as already evidenced in[22] for smaller samples of 250 molecules, the force field slightly overestimates the order of the β-δ $C-H$ bonds, but overall the agreement is satisfactory (especially for ν_α) considering the small differences in

8

temperature and solvent order parameter between the experimental and the simulated samples. Also for for rigid solutes dissolved in a nematic solvent, the most direct way of comparing the simulation results with experiment is via NMR observables, in this case dipolar couplings D_{ij} between nuclei i, j (typically ^{1}H or ^{13}C). In computer simulations these observables can be calculated directly from their definition:

$$D_{ij} = -\frac{\mu_0}{16\pi^2}\gamma_i\gamma_j\hbar\left\langle\frac{3\cos^2\theta_{ij}-1}{r_{ij}^3}\right\rangle \; , \tag{3}$$

$$= -\frac{\mu_0}{16\pi^2}\gamma_i\gamma_j\hbar\langle T_{ZZ}(r_{ij})\rangle \; . \tag{4}$$

where $\mathbf{r}_{ij}$ is the internuclear vector having an orientation θ_{ij} with respect to the spectrometer magnetic field $\mathbf{B}$ (in our case, parallel to phase director $\mathbf{n}$). We also have $\mu_0 = 4\pi \times 10^{-7}$T^{2}J^{-1}m^3, the magnetic permeability in vacuum; $\gamma_i = g_i\mu_N/\hbar$ the nuclear gyromagnetic ratio expressed in radiants, the nuclear factor g_i, characteristic of nucleus i, and the nuclear magneton $\mu_N = 5.051 \times 10^{-27}$JT^{-1}. If the molecule is rigid the internuclear distances r_{ij} are essentially constant (neglecting vibration fluctuations), the average in the last term can be approximated as $\left[\, 2\langle P_2(\cos\theta_{ij})\rangle\,/r_{ij}^3\,\right]$ which is geometrically related to $\langle P_2\rangle_S$ via a simple rotation. Eq. (3) indicates that the couplings D_{ij} depend only on the ZZ component of the averaged dipolar coupling tensor $\mathbf{T}(r_{ij})$ where, omitting the i,j subscripts:

$$\mathbf{T}(r) = \nabla\nabla\frac{1}{r} = \frac{1}{r^5}\begin{pmatrix} 3x^2 - r^2 & 3xy & 3xz \\ 3yx & 3y^2 - r^2 & 3yz \\ 3zx & 3zy & 3z^2 - r^2 \end{pmatrix} . \tag{5}$$

This is because the traceless tensor $\langle\mathbf{T}\rangle$, average over sample and the MD configurations, should be diagonal in the director frame with components $\langle T_{\mathrm{II}}\rangle$. For a uniaxial liquid crystal the two directions transversal to the director are equivalent and we have $\langle T_{\mathrm{XX}}\rangle = \langle T_{\mathrm{YY}}\rangle = -\frac{1}{2}\langle T_{\mathrm{ZZ}}\rangle$, hence

we can only consider the absolute value of the largest component $\langle T_{ZZ} \rangle$ (Eq. (3)). This can also used to validate the MD results and, by considering a sufficiently large number of statistically independent configurations (here ~ 4000), we find that these average off-diagonal terms range between 0.01% and 1% of the diagonal terms, and can be thus considered negligible.

It is interesting to note that the simulated D_{ij} values for our solutes in 5CB are in qualitative agreement with the experimental data obtained in other LC solvents,[46] and in particular they are similar to the values measured in ZLI 1132 (see Table 5). This is not surprising as the latter LC is a mixture of cyano-biphenyls and cyano-bicyclohexyls, hence it is rather similar to 5CB from a chemical point view. In Table 5 we have also reported the results obtained from simulations setting to zero the partial charges on the solute molecules and, as expected,[1] these couplings are more similar to the ones measured in the magic mixture.

In Table 6 we present similar results in terms of the ^{13}C dipolar couplings for the nematic solvent. The experimental values (measured at 301 K) must be considered as upper limits of the values simulated with solutes because they are measured for pure 5CB.[47] The simulated couplings are in good agreement with experiment, even if we can notice a small systematic underestimation, related to the slightly larger $\langle P_2 \rangle_{\mathrm{LC}}$ value of 0.53 measured in[47] with respect to $\langle P_2 \rangle_{\mathrm{LC}} = 0.50 \pm 0.02$ obtained from simulation. In Table 6 the average dipolar couplings for 5CB in presence of solutes are also reported. Considering the shift in transition temperature induced by the solutes we present here the data at 295 K, finding again a qualitative agreement with the experimental couplings of pure 5CB.

Comparison with theoretical models for alignment

The theoretical models developed in literature for the interpretation of solute alignment in a liquid crystalline solvent are tipically based on a mean field approach,[1,7,14,48,49] consisting in replacing the sum of explicit pair interactions between solute and solvent molecules with an effective anisotropic single-particle potential experienced by a solute and generated by the surrounding

molecules. To evaluate the performances of two popular theoretical models we have compared their predictions with our computer simulation results.

The model formulated by Maier and Saupe (MS)[30] originally developed for pure nematics was extended to mixtures as required for solute-solvent systems by Humphries, James and Luckhurst (HJL)[50] and was probably the first successful theory used in interpreting the experimental data on solute orientational order in a nematic liquid crystal solvent.[14] The MS orienting potential at low (strictly vanishingly small) solute concentrations is expressed for a rigid uniaxial solute as:

$$U_{\text{MS}}(\cos\beta) = \zeta\langle P_2\rangle_{\text{LC}}P_2(\cos\beta) \tag{6}$$

where ζ is the specific solute-solvent interaction strength, $\langle P_2\rangle_{\text{LC}}$ is the order parameter of the nematic solvent, and β the orientation of the solute axis with respect to the mesophase director. In the original MS theory ζ is determined by dispersive interactions, but in HJL more general formulation it collects all second rank interactions.[14] The parameter ζ assumes a different value for every solute-solvent; however in the MS and HJL theory it does not depend on temperature as long as the molecules are rigid and the intermolecular interactions can be considered constant, while the temperature enters indirectly via $\langle P_2\rangle_{\text{LC}}$. In our case we can check the predictions of this model by deriving an effective "a posteriori" potential acting on a molecule from the analysis of the MD configurations. For this purpose we have calculated average histograms of the orientational distribution function $\mathscr{P}(\cos\beta)$, giving the probability of observing a solute molecule at an orientation $\cos\beta \pm \Delta\cos\beta$ with respect to the director $\mathbf{n}$ during the MD simulation. From this $\mathscr{P}(\cos\beta)$ we can calculate an effective anisotropic potential energy U_{eff} as:[51]

$$U_{\text{eff}}(\cos\beta) = -k_BT\ln\mathscr{P}(\cos\beta) + U_0 \quad . \tag{7}$$

Where U_0 is a constant used for shifting the minimum value of $U_{\text{eff}}(\cos\beta)$ to zero.

We have plotted (see Figure 5) these energy histograms for the various solutes against the simple second rank profiles predicted by the MS model (6) after performing a global fitting of

11

the ζ parameter against all $U_{\text{eff}}(\cos\beta)$ obtained from MD at the various temperatures and using simulated solvent order parameters $\langle P_2 \rangle_{\text{LC}}$ reported in Table 1. To optimise the ζ values we have used the simplex algorithm[52] which is robust and adequate for this one-parameter minimisation of the weighted residual function:

$$\chi^2 = \sum_i \mathscr{P}(\cos\beta_i)[U_{\text{eff}}(\cos\beta_i) - U_{\text{MS or ST}}(\cos\beta_i)]^2 \quad , \tag{8}$$

where the sum runs over all the bins i of the simulated histogram of $\mathscr{P}(\cos\beta)$.

For the analysis of these results (see Table 7) we consider two different groups of solutes: the prolate molecules (ACE, PRO and ACN) and the oblate ones (BEN and TBB), both with standard and chargeless modelling of the electrostatic interactions. For the first three solutes we obtain quite similar ζ values ($\zeta < -0.7$) and a low ($\sim 6\%$) rms error, confirming the functional form (6) with the temperature dependence of the effective potential confined to that of $\langle P_2 \rangle_{\text{LC}}$.[53] For the two oblate molecules (with similar form) the optimisation gives an effective interaction strength $\zeta > 1.3$ with a rms error $\sim 6\%$. This value is larger than that obtained for our prolate solutes. Given the second rank nature of the effective potential, i.e. $-U(\cos\beta)/(k_B T) = a_2 P_2(\cos\beta)$ with $a_2 = \zeta \langle P_2 \rangle_{\text{LC}}/(k_B T)$, a simple analytical approximation[54] relating a_2 to the order parameter gives $\langle P_2 \rangle_{\text{LC}} = a_2/\zeta$ predicting a linear relation between solute and solvent order, verified e. g. in the reference 1,3,5-trichlorobenzene (Figure 2).

Interestingly, we find that the optimised ζ values are quite comparable for standard and chargeless solutes. This result hints that the electrostatic interactions and in particular quadrupolar ones play a secondary role in determining the orientational distribution of these solutes in the LC solvent, as already evidenced in the discussion of the solute order parameter (Table 2) and suggested in previous studies .[15,55]

Another model proposed to explain solute alignment in nematics is the surface tensor (ST) one, which[31] assumes that the unit vector $\mathbf{k}$ perpendicular to each infinitesimal surface element dS of a molecule tends to orient perpendicularly to the director $\mathbf{n}$. The molecular orientation β is then governed by an energy given by the integral over all elements dS defining the molecular surface S:

$$U_{ST}(\cos\beta) = \varepsilon \int_S \left[\frac{3}{2}(\mathbf{k}\cdot\mathbf{n})^2 - \frac{1}{2} \right] dS \ , \tag{9}$$

where ε is a temperature-dependent interaction strength, which should take the same value for all solutes in a given solvent. To compare the predictions of this model with our MD results we have first proceeded, following Ferrarini et al.,[31] with calculating numerically the molecular surface for each solute and the ratio U_{ST}/ε, which is a function of molecular shape only. The molecular shape has been described as a collection of spheres each having the Lennard Jones radius used in the AMBER-OPLS force field,[37,38] and using the B3LYP//6-31G** equilibrium geometry for their positions. To derive a more manageable expression, the integral in 9 has been approximated for our uniaxial solutes as a truncated series expansion in Legendre polynomials with even coefficients:

$$U_{ST}(\cos\beta)/\varepsilon \simeq \sum_{L=0}^{3} a_{2L} P_{2L}(\cos\beta) \tag{10}$$

where the a_{2L} parameters are solute-specific geometrical constants. In Table 8 we report these coefficients, as well as the corresponding surfaces S and their projection along the molecular principal axes. We see from Table 8 that for all solutes the second rank coefficient a_2 is largely dominant. Thus, the functional form of U_{MS} and U_{ST} are effectively the same if we consider only one solute and one temperature. However we may hope to distinguish between the two models analyzing various sets of data together i. e. performing a "global fit".[56] In this way we can test ζ to be solute dependent and temperature independent and a_2 to change with temperature but to be solute independent.

The profiles $U_{ST}(\cos\beta)/\varepsilon$ of 10 are shown in Figure 6 plate A, while in plate B these energies are normalised by their corresponding value of S to compare more easily the results for different solutes. We notice first that also the ST model discriminates in all cases between oblate and prolate molecules and also that it correctly allows to associate the orienting effects due to shape anisotropy in the case of molecules with different dimensions (for example propyne or acetonitrile with respect to acetylene, see Figure 6 plate B). The behavior of ACE is particularly revealing, as it shows a

13

$U_{ST}(\cos\beta)/\varepsilon$ profile similar to propyne, but a different energy per area $U_{ST}(\cos\beta)/(\varepsilon S)$. This implies that even if the interaction with solvent per unit surface of acetylene is lower than for propyne, the larger surface of acetylene molecule determines a total interaction energy comparable to propyne.

The $U_{eff}(\cos\beta)$ profiles from the MD simulations have been fitted using the ST model both in a single-solutes fashion and with a global approach to obtain a universal ε coefficient for all solutes at a given temperature. Again, all these optimisations have been performed with the simplex algorithm. The results are given in Table 9 and we see that for every temperature the values of ε obtained from the single-solute analyses are quite scattered with respect to the global one obtained fitting simultaneously all $U_{eff}(\cos\beta)$ profiles, even if they present ST $\varepsilon/(k_B T)$ values in the nematic phase ranging from 0.036 Å^{-2} (1,3,5 tribromobenzene at 295 K), to 0.109 Å^{-2} (acetonitrile at 285 K) and thus appear to be roughly in the range of 0.04 $\text{Å}^{-2} < \varepsilon/(k_B T) < 0.07$ Å^{-2} given by Ferrarini et al.[57,58]

It should also be taken into account that the absolute value of the molecular surface depends on the method of calculating it, and that this can affect the range of the $\varepsilon/(k_B T)$ parameter.

The resulting $U_{ST}(\cos\beta)$ energy curves are plotted in Figure 7 against the $U_{eff}(\cos\beta)$ histograms for the $T = 295$ K case. We see that the $U_{ST}(\cos\beta)$ profiles do not reproduce well the MD data and quite revealingly the ST model performs slightly better with the results obtained for the chargeless solutes. This is not surprising considering that the surface tensor model only attempts to take into account orienting effects arising from the anisotropic shape of the solutes while solute-solvent interaction contributions are included only in the generic ε parameter. Even though the MS model outperforms the ST one, it should be noted that the MS it is only apparently a one-parameter model since $\langle P_2 \rangle_{LC}$ provides an additional (albeit indirect and empirical) source of information that takes correctly into account the temperature dependence of the data. These results support the view that a complete modelling of solutes orientation in LC solvents should consider both anisotropic shape and interaction effects.[48,59]

It is somewhat surprising that switching off the charges of the solutes has a relatively small

effect on their order (Table 2) not only of the apolar molecules like benzene but even for acetonitrile (ACN) notwithstanding its CN group and a dipole moment of $\sim 4D$ (see Supporting Information). To examine this point, we have calculated the radial and polar pair correlations between the CN group of the solute (ACN) and the solvent (5CB):

$$g_0^{CN-CN}(r) = \frac{1}{4\pi r^2 \rho_N} \langle \delta \left(r - r_{ij} \right) \rangle_{ij} \tag{11}$$

$$g_1^{CN-CN}(r) = \langle \delta \left(r - r_{ij} \right) \left(\mathbf{u}_i \cdot \mathbf{u}_j \right) \rangle_{ij} \tag{12}$$

where r_{ij} is the distance between the midpoint of the CN bonds of ACN and 5CB. We see the results for g_0 and g_1 in Figure 8A, Figure 8B for the two cases of solute charges on and off at $T = 285$ K. We observe that indeed at short range the solvent around ACN becomes less structured on switching off charges (the second peak dissapears). As for the relative orientation of ACN and 5CB, we see from g_1 that they are on average antiparallel and that eliminating the charges the association becomes weaker as indicated by the decrease of the first peak.

Thus we see that the effects are mainly concentrated on the short range order, while the long range which is relatively independent from the local structure[53] does not seem to depend on the local effects.

Conclusions

We have studied with atomistic molecular dynamics simulations the orientational order of small rigid uniaxial solutes dissolved in the nematic liquid-crystal phase of 5CB. We have employed rather large (N = 2000) samples with the solutes described at full atomistic detail and the solvent at united atoms level. For determining the effect of the electrostatic contributions of the inter-molecular potential on solute orientational order, we have performed two sets of simulations: one with partial atomic charges of solutes present and one where these have been switched off.

We noticed that the presence of a solute can modify the order within the liquid-crystal phase and in our case a decrease of the nematic-isotropic transition temperature from 308 K to 300 K is observed. Simulations correctly predict the ordering effect of the LC solvent on solutes, yelding a good agreement between the computed order parameters and dipolar couplings and the ones measured in NMR experiments, where these are available. Our results validate for the first time the use of atomistic MD as a mean of predicting solute order at concentrations similar to those used in NMR and this in turn should open the way to a better understanding of the physical origin of solute alignment.

The orientational distribution functions of solutes were compared with the theoretical predictions of the surface tensor model[31] and the mean field Maier-Saupe type model of Humphries, James and Luckhurst [50] for checking their validity; the surface tensor model appears to provide only qualitative previsions; the Maier-Saupe model instead is capable of reproducing the potential energy curves for all solutes.

The applicability of mean field models to the simulation results and the very limited effect of solute charges on the orientational order, indicate that the alignment mechanism in 5CB, at least for our solutes, is dominated by repulsive and van der Waals interactions.

Acknowledgement

Supporting Information Available

Atom label and charges, dipoles and quadrupoles for all the compounds studied; Complete reference no. 34. This information is available free of charge via the Internet at http://pubs.acs.org.

References

(1) Burnell, E. E.; Lange, C. A. D. *Chem. Rev.* **1998**, *98*, 2359–2387.

(2) Burnell, E. E., de Lange, C. A., Eds. *NMR of Ordered Liquids*; Kluwer: Dordrecht, 2003.

(3) Emsley, J. W.; Lindon, J. C. *NMR Spectroscopy using Liquid Crystal Solvents*; Pergamon Press: Oxford, 1976.

(4) Emsley, J. W. *Nuclear Magnetic Resonance of Liquid Crystal*; Reidel: Dordrecht, 1985.

(5) Khetrapal, C. L.; Gowda, G. A. N.; Ramanathan, K. V. *Nuclear Magnetic Resonance*; The Royal Society of Chemistry: Cambridge, 2002; Vol. 31.

(6) Bax, A.; Grishaev, A. *Curr. Opin. Struct. Biol.* **2005**, *15*, 563–570.

(7) Luckhurst, G. R., Veracini, C. A., Eds. *The Molecular Dynamics of Liquid Crystals*; Kluwer: Dordrecht, 1989.

(8) Celebre, G.; Luca, G. D.; Longeri, M.; Catalano, D.; Veracini, C. A.; Emsley, J. W. *J. Chem. Soc. Faraday Trans.* **1991**, *87*, 2623–2627.

(9) Celebre, G.; Luca, G. D.; Longeri, M. *Liq. Cryst.* **2010**, *37*, 923–933.

(10) Saupe, A.; Englert, G. *Phys. Rev. Lett.* **1963**, *11*, 462–464.

(11) Burnell, E. E.; Berardi, R.; Syvitski, R. T.; Zannoni, C. *Chem. Phys. Lett.* **2000**, *331*, 455 – 464.

(12) Lee, J. S. J.; Sokolovskii, R. O.; Berardi, R.; Zannoni, C.; Burnell, E. E. *Chem. Phys. Lett.* **2008**, *454*, 56–60.

(13) Sokolovskii, R. O.; Burnell, E. E. *J. Chem. Phys.* **2009**, *130*, 154507.

(14) Catalano, D.; Forte, C.; Veracini, C. A.; Zannoni, C. *Isr. J. Chem.* **1983**, *23*, 283–389.

(15) Dingemans, T.; Photinos, D. J.; Samulski, E. T.; Terzis, A. F.; Wutz, C. *J. Chem. Phys.* **2003**, *118*, 7046–7061.

(16) Danilovic, Z.; Burnell, E. E. *J. Chem. Phys.* **2009**, *130*, 154506.

(17) Celebre, G.; Luca, G. D. *J. Phys. Chem. B* **2003**, *107*, 3243–3250.

(18) Celebre, G.; Ionescu, A. *J. Phys. Chem. B* **2010**, *114*, 235–241.

(19) Celebre, G.; Luca, G. D. *Chem. Phys. Lett.* **2003**, *368*, 359–364.

(20) Celebre, G.; Ionescu, A. *J. Phys. Chem. B* **2010**, *114*, 228–234.

(21) Picken, S. J.; de Jeu, W. H. *Liq. Cryst.* **2006**, *33*, 1359–1362.

(22) Tiberio, G.; Muccioli, L.; Berardi, R.; Zannoni, C. *ChemPhysChem* **2009**, *10*, 125–136.

(23) Berardi, R.; Muccioli, L.; Zannoni, C. *ChemPhysChem* **2004**, *5*, 104.

(24) Pelaez, J.; Wilson, M. R. *Phys. Rev. Lett.* **2006**, *97*, 267801.

(25) Cacelli, I.; Gaetani, L. D.; Prampolini, G.; Tani, A. *J. Phys. Chem. B* **2007**, *111*, 2130–2137.

(26) Pizzirusso, A.; Savini, M.; Muccioli, L.; Zannoni, C. *J. Mat. Chem.* **2011**, *21*, 125–133.

(27) Pizzirusso, A.; Berardi, R.; Muccioli, L.; Ricci, M.; Zannoni, C. *Chem. Sci.* **2012**, *3*, 573–579.

(28) Burnell, E. E.; de Lange, C. A.; Meerts, W. L. In *Nuclear Magnetic Resonance Spectroscopy of Liquid Crystals*; Dong, R. Y., Ed.; World Scientific: Singapore, 2010; pp 1–36.

(29) de Lange, C. A.; Meerts, W. L.; Weber, A.; Burnell, E. E. *J. Phys. Chem. A* **2010**, *114*, 5878–5887.

(30) Straley, J. P. *Phys. Rev. A* **1974**, *10*, 1881–1887.

(31) A. Ferrarini, P. L. N., G. R. Luckhurst; Roskilly, S. J. *J. Chem. Phys.* **1994**, *100*, 1460–1469.

(32) Zannoni, C. In *The Molecular Physics of Liquid Crystals*; Luckhurst, G. R., Gray, G. W., Eds.; Academic Press: London, 1979; Chapter 3, pp 51–83.

(33) Besler, B. H.; Jr., K. M. M.; Kollman, P. A. *J. Comput. Chem.* **1990**, *11*, 431–439.

(34) Frisch, M. J.; Trucks, G. W.; Schlegel, H. B.; Scuseria, G. E.; Robb, M. A.; Cheeseman, J. R.; Montgomery, J. A., Jr.; Vreven, T.; Kudin, K. N.; Burant, J. C.; Millam, J. M. et al. Gaussian 03, Revision C.02. Gaussian, Inc., Wallingford, CT, 2004.

(35) Phillips, J. C.; Braun, R.; Wang, W.; Gumbart, J.; Tajkhorshid, E.; Villa, E.; Chipot, C.; Skeel, R. D.; Kale, L.; Schulten, K. *J. Comput. Chem.* **2005**, *26*, 1781–1802.

(36) Berendsen, H. J. C.; Postma, J. P. M.; van Gunsteren, W. F.; Nola, A. D.; Haak, J. R. *J. Chem. Phys.* **1984**, *81*, 3684–3690.

(37) Cornell, W. D.; Cieplak, P.; Bayly, C. I.; Gould, I. R.; Merz, K. M.; Ferguson, D. M.; Spellmeyer, D. C.; Fox, T.; Caldwell, J. W.; Kollman, P. A. *J. Am. Chem. Soc.* **1995**, *117*, 5179–5197.

(38) J. Wang, P. C.; Kollman, P. A. *J. Comput. Chem.* **2000**, *21*, 1049–1074.

(39) Essmann, U.; Perera, L.; Berkowitz, M. L.; Darden, T. A.; Lee, H.; Pedersen, L. G. *J. Chem. Phys.* **1995**, *103*, 8577–8593.

(40) Vecchi, I.; Arcioni, A.; Bacchiocchi, C.; Tiberio, G.; Zanirato, P.; Zannoni, C. *J. Phys. Chem. B* **2007**, *111*, 3355–3362.

(41) Guo, W.; Fung, B. M. *Liq. Cryst.* **1991**, *9*, 117–126.

(42) Luckhurst, G. R.; Gray, G. W. *The Molecular Physics of Liquid Crystals*; Academic Press: London, 1979.

(43) Weaver, A.; der Est, A. V.; Rendell, J.; Hoatson, G.; Bates, G.; Burnell, E. E. *Liq. Cryst.* **1987**, *2*, 633–642.

(44) Auger, C.; Lesage, A.; Caldarelli, S.; Hodgkinson, P.; Emsley, L. *J. Phys. Chem. B* **1998**, *102*, 3718–3723.

(45) Emsley, J. W.; Luckhurst, G. R.; Stockley, C. P. *Mol. Phys.* **1981**, *44*, 565–580.

(46) der Est, A. V.; Kok, M.; Burnell, E. *Mol. Phys.* **1987**, *60*, 397–413.

(47) Sandström, D.; Levitt, M. H. *J. Am. Chem. Soc.* **1996**, *118*, 6966–6974.

(48) Matteo, A. D.; Ferrarini, A.; Moro, G. J. *J. Phys. Chem. B* **2000**, *104*, 7764–7773.

(49) Luckhurst, G. R.; Zannoni, C.; Nordio, P. L.; Segre, U. *Mol. Phys.* **1975**, *30*, 1345–1358.

(50) Humphries, R. L.; James, P. G.; Luckhurst, G. R. *Symp. Faraday Soc.* **1971**, *5*, 107–118.

(51) Luckhurst, G. R. In *The Molecular Physics of Liquid Crystals*; Luckhurst, G. R., Gray, G. W., Eds.; Academic Press: London, 1979; Chapter 4, pp 85–119.

(52) Nelder, J. A.; Mead, R. *Comput. J.* **1965**, *7*, 308–313.

(53) Luckhurst, G. R.; Zannoni, C. *Nature* **1977**, *267*, 412–415.

(54) Fabbri, U.; Zannoni, C. *Mol. Phys.* **1986**, *58*, 763–788.

(55) Williams, V. E.; Lemieux, R. P. *J. Am. Chem. Soc.* **1998**, *120*, 11311–11315.

(56) Arcioni, A.; Tarroni, R.; Zannoni, C. *J. Chem. Soc. Faraday Trans.* **1993**, *89*, 2815–2822.

(57) Ferrarini, A.; Moro, G. J.; Nordio, P. L.; Luckhurst, G. R. *Mol. Phys.* **1992**, *77*, 1–15.

(58) Ferrarini, A.; Moro, G. J.; Nordio, P. L. *Phys. Rev. E* **1996**, *53*, 681–688.

(59) Matteo, A. D.; Ferrarini, A.; Moro, G. J.; Celebre, G.; Luca, G. D.; Longeri, M. *Mol. Cryst. Liq. Cryst.* **2002**, *A 372*, 107–120.

Table 1: Order parameters $\langle P_2 \rangle_{\mathrm{LC}}$ of 5CB (referred to the inertial tensor principal axis) as a function of temperature from MD simulations of solutions with standard charges (^{q}) and immediately below deviations $\delta \langle P_2 \rangle_{\mathrm{LC}}$ obtained in presence of chargeless solutes (^{0}). The respective values of T_{NI} are also reported.

solvent	285 K	290 K	295 K	300 K	305 K	T_{NI} (K)
BEN^q	0.66 ± 0.02	0.62 ± 0.02	0.54 ± 0.04	0.18 ± 0.06	0.15 ± 0.06	300
δ_{BEN}^0	0.00 ± 0.02	-0.01 ± 0.03	$+0.02 \pm 0.02$	-0.06 ± 0.05	-0.03 ± 0.07	300
TBB^q	0.63 ± 0.02	0.59 ± 0.03	0.49 ± 0.04	0.18 ± 0.12	0.08 ± 0.04	300
δ_{TBB}^0	-0.03 ± 0.03	-0.03 ± 0.03	-0.08 ± 0.05	$+0.01 \pm 0.08$	$+0.01 \pm 0.04$	300
ACE^q	0.66 ± 0.02	0.64 ± 0.03	0.58 ± 0.04	0.15 ± 0.07	0.13 ± 0.04	300
δ_{ACE}^0	$+0.01 \pm 0.02$	-0.01 ± 0.03	-0.01 ± 0.03	$+0.29 \pm 0.08$	-0.02 ± 0.03	305
PRO^q	0.67 ± 0.02	0.62 ± 0.02	0.56 ± 0.02	0.35 ± 0.09	0.10 ± 0.03	305
δ_{PRO}^0	-0.02 ± 0.03	$+0.01 \pm 0.02$	-0.02 ± 0.05	$+0.15 \pm 0.04$	$+0.12 \pm 0.11$	305
ACN^q	0.66 ± 0.02	0.63 ± 0.02	0.57 ± 0.03	0.42 ± 0.05	0.08 ± 0.02	305
δ_{ACN}^0	0.00 ± 0.02	-0.02 ± 0.02	-0.02 ± 0.05	-0.02 ± 0.05	$+0.02 \pm 0.05$	305

Table 2: Order parameters $\langle P_2 \rangle_{\mathrm{S}}$ for rigid solutes from the MD simulations considering the electrostatic solute-solvent interactions (^{q}) and below each value the deviations from these $\delta \langle P_2 \rangle_{\mathrm{S}}$ neglecting the electrostatic contributions (^{0}).

solute	285 K	290 K	295 K	300 K	305 K
BEN^q	-0.25 ± 0.04	-0.23 ± 0.04	-0.19 ± 0.04	-0.06 ± 0.05	-0.05 ± 0.05
δ_{BEN}^0	$+0.02 \pm 0.04$	$+0.02 \pm 0.04$	$+0.01 \pm 0.04$	$+0.02 \pm 0.05$	$+0.01 \pm 0.05$
TBB^q	-0.26 ± 0.04	-0.24 ± 0.04	-0.20 ± 0.04	-0.08 ± 0.07	-0.04 ± 0.05
δ_{TBB}^0	$+0.01 \pm 0.04$	$+0.01 \pm 0.04$	$+0.03 \pm 0.05$	0.00 ± 0.06	0.00 ± 0.05
ACE^q	0.19 ± 0.05	0.18 ± 0.05	0.15 ± 0.05	0.03 ± 0.05	0.03 ± 0.05
δ_{ACE}^0	-0.07 ± 0.05	-0.07 ± 0.05	-0.05 ± 0.05	$+0.04 \pm 0.05$	-0.02 ± 0.05
PRO^q	0.24 ± 0.05	0.21 ± 0.06	0.18 ± 0.05	0.10 ± 0.06	0.03 ± 0.05
δ_{PRO}^0	-0.08 ± 0.05	-0.06 ± 0.05	-0.06 ± 0.05	0.00 ± 0.05	$+0.01 \pm 0.06$
ACN^q	0.20 ± 0.05	0.18 ± 0.06	0.15 ± 0.05	0.11 ± 0.05	0.02 ± 0.05
δ_{ACN}^0	-0.06 ± 0.05	-0.06 ± 0.05	-0.05 ± 0.05	-0.04 ± 0.05	-0.01 ± 0.05

Table 3: Comparison of the experimental order parameters $\langle P_2 \rangle_S$ for solutes in 5CB at 294 K (taken from ref. [43]) with those calculated from MD simulations at 295 K. [*] Experimental order parameters for benzene in 5CB at 296 K. [43]

solute	$\langle P_2 \rangle_S$ (exp)	$\langle P_2 \rangle_S$ (sim)
BEN*	-0.14 ± 0.05	-0.19 ± 0.04
TBB	-0.22 ± 0.05	-0.20 ± 0.04
ACE	0.17 ± 0.05	0.15 ± 0.05
PRO	0.17 ± 0.05	0.18 ± 0.05

Table 4: Experimental absolute values of the ^{2}H quadrupolar splittings ($|\Delta\nu'|$) for the hydrogens belonging to 5CB alkyl chain (in kHz) measured for pure solvent [44] and in solutions, [43] and average values calculated in this work ($\Delta\nu$). The position in the alkyl chain is indicated with greek letters, with α–γ being the first–fourth methylene groups and ω corresponding to the terminal methyl group.

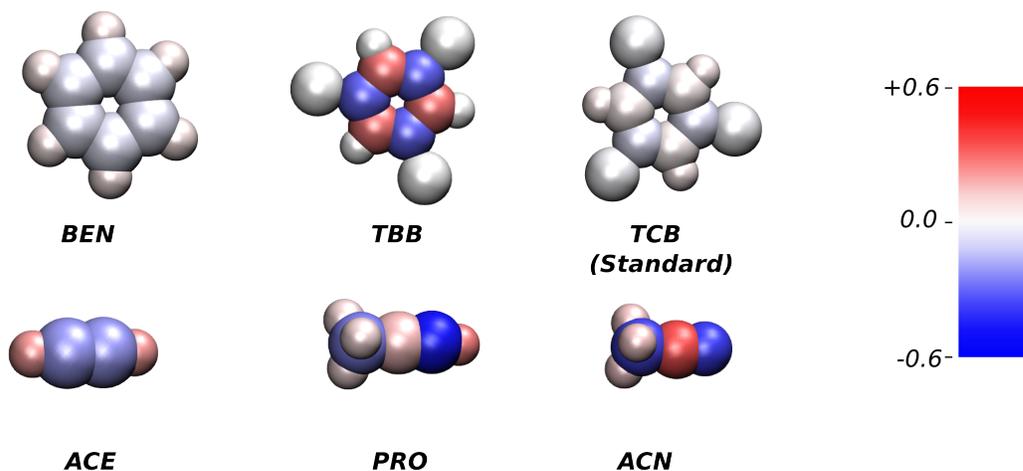| solvent	T (K)	$|\Delta\nu'_\alpha|$	$|\Delta\nu'_\beta|$	$|\Delta\nu'_\gamma|$	$|\Delta\nu'_\delta|$	$|\Delta\nu'_\omega|$	T (K)	$\Delta\nu_\alpha$	$\Delta\nu_\beta$	$\Delta\nu_\gamma$	$\Delta\nu_\delta$	$\Delta\nu_\omega$
5CB$_{BEN}$	296	44.0	29.5	-	-	-	295	-51.9	-44.0	-44.5	-35.5	-11.0
5CB$_{TBB}$	294	50.1	34.2	-	-	-	295	-47.5	-40.1	-40.7	-32.3	-9.5
5CB$_{ACE}$	294	58.1	41.2	-	-	-	295	-56.5	-48.1	-48.6	-38.9	-13.7
5CB$_{PRO}$	294	53.2	36.6	-	-	-	295	-54.0	-45.9	-46.4	-36.9	-16.4
5CB$_{ACN}$	-	-	-	-	-	-	295	-54.8	-46.5	-47.1	-37.6	-14.4
5CB	299	51.8	35.4	37.9	25.3	18.3	300	-50.5	-42.6	-43.1	-34.0	-13.5

Figure 1: Spacefilling representations of the oblate (top) and prolate (bottom) solutes studied in this work: benzene (BEN), 1,3,5-tribromobenzene (TBB), 1,3,5-trichlorobenzene (TCB), acetylene (ACE), propyne (PRO) and acetonitrile (ACN). Atoms are color-coded according to their partial charges obtained from an energy minimization using the B3LYP density functional and the $6-31G^{**}$ basis set. [34] The colors range from blue ($e = -0.6$) to red ($e = +0.6$). See Supporting Information for additional details.

Table 5: Mean solute dipolar couplings (in Hz) from[46] measured at $T = 301.4$ K in nematic solvents 1132, EBBA and their "magic mixture", and from our simulations in 5CB (D_T, in Hz) with standard (^{q}) and chargeless (^{0}) solutes. The liquid crystal solvent defined as "magic mixture" is composed of 55 wt% 1132 and 45 wt% EBBA. See Figures in Supporting Information for atom labels.

Molecule	Nuclei	1132	"magic"	EBBA	$D_{285\ K}$	$D_{290\ K}$	$D_{295\ K}$	$D_{300\ K}$
BEN^q	H2-H4,H12;H6-H4,H8;	-987.99	-708.47	-461.48	-966	-898	-747	-244
BEN^0	H10-H8,H12				-910	-821	-727	-161
BEN^q	H2-H6,H10; H6-H10;	-191.73	-137.15	-88.46	-187	-173	-144	-47
BEN^0	H4-H8,H12; H8-H12				-175	-158	-140	-31
BEN^q	H2-H8;H4-H10;	-125.05	-89.32	-57.34	-121	-112	-94	-30
BEN^0	H6-H12				-114	-103	-91	-20
TBB^q	H2-H6,H10;	-213.56	-159.2	-119.90	-194	-179	-151	-58
TBB^0	H6-H10				-186	-171	-125	-57
ACE^q	H3-H4	-644.6	-298.56	145.8	-639	-586	-496	-106
ACE^0					-405	-373	-322	-231
ACE^q	C1-H3; C2-H4	-4763.2	-2131.23	1075.1	-4764	-4368	-3693	-789
ACE^0					-3024	-2788	-2404	-1722
ACE^q	C1-H4; C2-H3	-506.3	-234.73	114.9	-512	-468	-397	-84
ACE^0					-324	-299	-258	-184
ACE^q	C1-C2	-834.6	-389.4	180.2	-879	-806	-681	-145
ACE^0					-554	-511	-442	-316
PRO^q	H5-H4,H6; H4-H6	2853.10	1656.75	595.23	2556	2202	1871	1031
PRO^0					1675	1566	1227	1082
PRO^q	H7-H4,H5,H6	-401.43	-232.89	-82.47	-360	-310	-264	-145
PRO^0					-233	-218	-171	-151

Table 6: Average carbon-carbon dipolar couplings (in Hz) of 5CB solvent, obtained by means of MD simulation of N=2000 5CB at 300 K and for MD solution of studied solutes in 5CB at 295 K, to be compared to the experimental values obtained for pure 5CB at 301 ± 1 K.[47] See Figures in Supporting Information for atom labels.

carbons	exp.[47]	5CB	5CB$_{BEN}$	5CB$_{TBB}$	5CB$_{ACE}$	5CB$_{PRO}$	5CB$_{ACN}$
C2-C3	-	-1373	1148	-1051	-1249	-1540	-1557
C2-C4,C8	-175	-163	-162	-149	-177	-184	-186
C2-C5,C7	-67	-61	-61	-56	-66	-69	-69
C2-C6	-57	-49	-49	-45	-53	-55	-56
C2-C9	-	-20	-21	-19	-23	-23	-23
C2-C10	-	-12	-13	-12	-14	-14	-15
C2-C11,C13	-	-7	-7	-7	-8	-8	-8
C2-C12	-	-6	-6	-5	-7	-7	-7
C3-C4,C8	126	124	137	123	154	144	146
C3-C5,C7	-177	-160	-173	-159	-188	-180	-182
C3-C6	-183	-162	-175	-160	-190	-182	-184
C3-C9	-54	-46	-52	-48	-57	-54	-55
C3-C10,C14	-27	-24	-27	-25	-30	-28	-29
C3-C11,C13	-	-12	-14	-12	-15	-14	-14
C3-C12	-	-10	-11	-10	-12	-11	-12
C4-C5,C7-C8	-1444	-1297	-1410	-1291	-1534	-1469	-1486
C6-C4,C8	-174	-160	-173	-159	-188	-180	-182
C4-C7,C5-C8	-	15	17	15	19	17	18
C4-C8	127	117	128	117	141	134	136
C9-C4,C8	-63	-57	-64	-59	-70	-67	-68
C4,C8-C10,C14	-34	-31	-35	-32	-38	-36	-37
C4,C8-C11,C13	-19	-23	-26	-24	-28	-27	-27
C4,C8-C12	-	-12	-14	-12	-15	-14	-14
C5,C7-C6	-	114	124	111	139	130	132
C5-C7	130	117	128	116	140	133	135
C9-C5,C7	-169	-152	-173	-158	-188	-180	-182
C5,C7-C10,C14	-87	-74	-84	-77	-91	-87	-88
C5,C7-C11,C13	-34	-31	-35	-32	-38	-36	-37
C12-C5,C7	-	-24	-27	-25	-30	-28	-29
C6-C9	-1224	-1120	-1416	-1297	-1541	-1476	-1492
C6-C10,C14	-170	-152	-172	-158	-187	-180	-182
C6-C11,C13	-63	-56	-64	-59	-70	-67	-68
C6-C12	-50	-46	-52	-47	-56	-54	-55
C9-C10,C14	-	118	129	115	143	134	137
C9-C11,C13	-177	-159	-172	-157	-187	-179	-181
C9-C12	-181	-160	-173	-158	-188	-180	-182
C10-C11,C13-C14	-1415	-1290	-1404	-1286	-1527	-1463	-1480
C12-C10,C14	-	-158	-172	-157	-186	-179	-181
C10-C13,C11-C14	-	16	18	16	20	18	19
C10-C14	131	119	130	118	142	135	137
C11-C13	132	119	130	118	142	135	137
C12-C11,C13	139	123	136	122	151	142	144

Table 7: The mean field solute-solvent interaction parameter ζ (see 6) obtained from the global fitting of the MD orientational energies (see 7) for various solutes at all simulated temperatures, and root mean square error (units of kcal mol^{-1}). The $\langle P_2 \rangle_{\mathrm{LC}}$ values used for the optimisation are those of Table 1.

	Standard		Chargeless	
Solute	ζ	RMSE	ζ	RMSE
BEN	1.33	0.08	1.23	0.06
TBB	1.54	0.06	1.49	0.07
ACE	-0.72	0.05	-0.47	0.05
PRO	-0.87	0.04	-0.61	0.05
ACN	-0.74	0.04	-0.51	0.06

Table 8: Total molecular surface S (Å^2) and the surface projections with respect to the three molecular axes, calculated using the method of Ferrarini *et al*,[31] and fit parameters of 10.

Solute	S	S_{XX}	S_{YY}	S_{ZZ}	a_0	a_2	a_4	a_6
BEN	117	57	30	29	-0.001	27.32	-0.010	-0.0151
TBB	187	85	50	50	-0.001	35.11	-0.013	-0.0217
ACE	57	23	23	10	0.000	-12.48	-0.002	-0.0028
PRO	80	31	30	18	-0.001	-11.84	-0.008	-0.0136
ACN	74	27	27	19	0.000	-8.15	0.002	0.0035

Table 9: The surface tensor model ε parameter (in kcal Å^{-2} mol^{-1}) and RMSE obtained by fitting the $U_{\mathrm{eff}}(\cos \beta)$ profiles from the MD data with the surface tensor model of 10 both from solutes with charges (^{q}) and chargeless ones (^{0}).

|	285 K		290 K		295 K		300 K		305 K	
solute	ε	RMSE	ε	RMSE	ε	RMSE	ε	RMSE	ε	RMSE
BEN^q	0.035	0.025	0.032	0.027	0.025	0.032	0.007	0.075	0.005	0.114
TBB^q	0.029	0.030	0.026	0.024	0.021	0.031	0.007	0.076	0.003	0.150
ACE^q	0.040	0.027	0.037	0.025	0.032	0.032	0.007	0.094	0.006	0.139
PRO^q	0.052	0.022	0.046	0.025	0.040	0.026	0.023	0.032	0.006	0.140
ACN^q	0.062	0.027	0.058	0.029	0.050	0.033	0.037	0.031	0.006	0.196
global^q	0.036	0.153	0.032	0.152	0.026	0.167	0.009	0.286	0.004	0.201
BEN^0	0.032	0.030	0.028	0.035	0.024	0.036	0.005	0.114	0.004	0.139
TBB^0	0.027	0.031	0.025	0.030	0.017	0.039	0.007	0.067	0.004	0.142
ACE^0	0.026	0.034	0.024	0.032	0.021	0.036	0.016	0.050	0.003	0.233
PRO^0	0.035	0.032	0.033	0.030	0.027	0.039	0.024	0.044	0.010	0.102
ACN^0	0.044	0.045	0.038	0.040	0.034	0.038	0.023	0.050	0.005	0.280
global^0	0.030	0.095	0.027	0.091	0.021	0.138	0.008	0.285	0.004	0.221
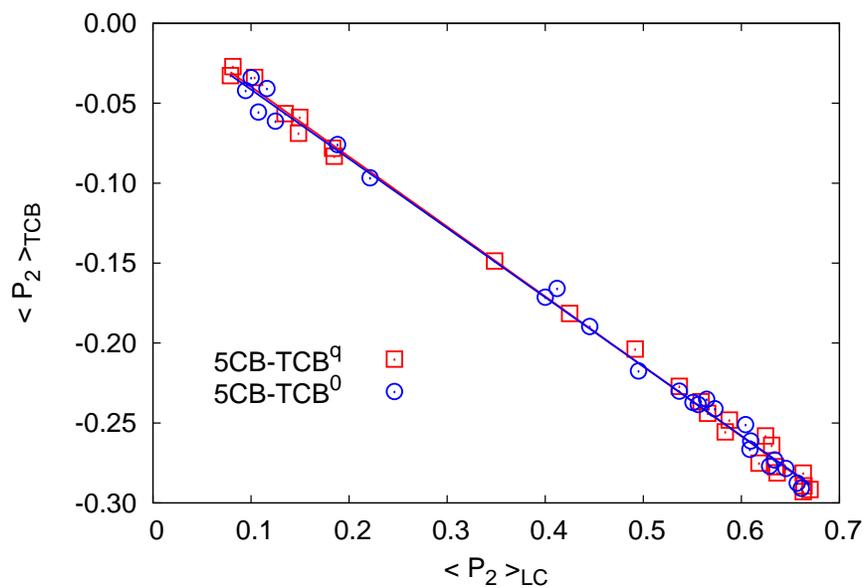
Figure 2: Orientational order parameters of the standard 1,3,5-trichlorobenzene $\langle P_2 \rangle_{\text{TCB}}$ plotted against the corresponding ones $\langle P_2 \rangle_{\text{LC}}$ for the 5CB solvent. Data are relative to MD simulation with standard (5CB-TCB^q, squares) and chargeless (5CB-TCB^0, circles) solute. The least square linear fits give in both cases a slope of about -0.43 and an intercept at the origin.
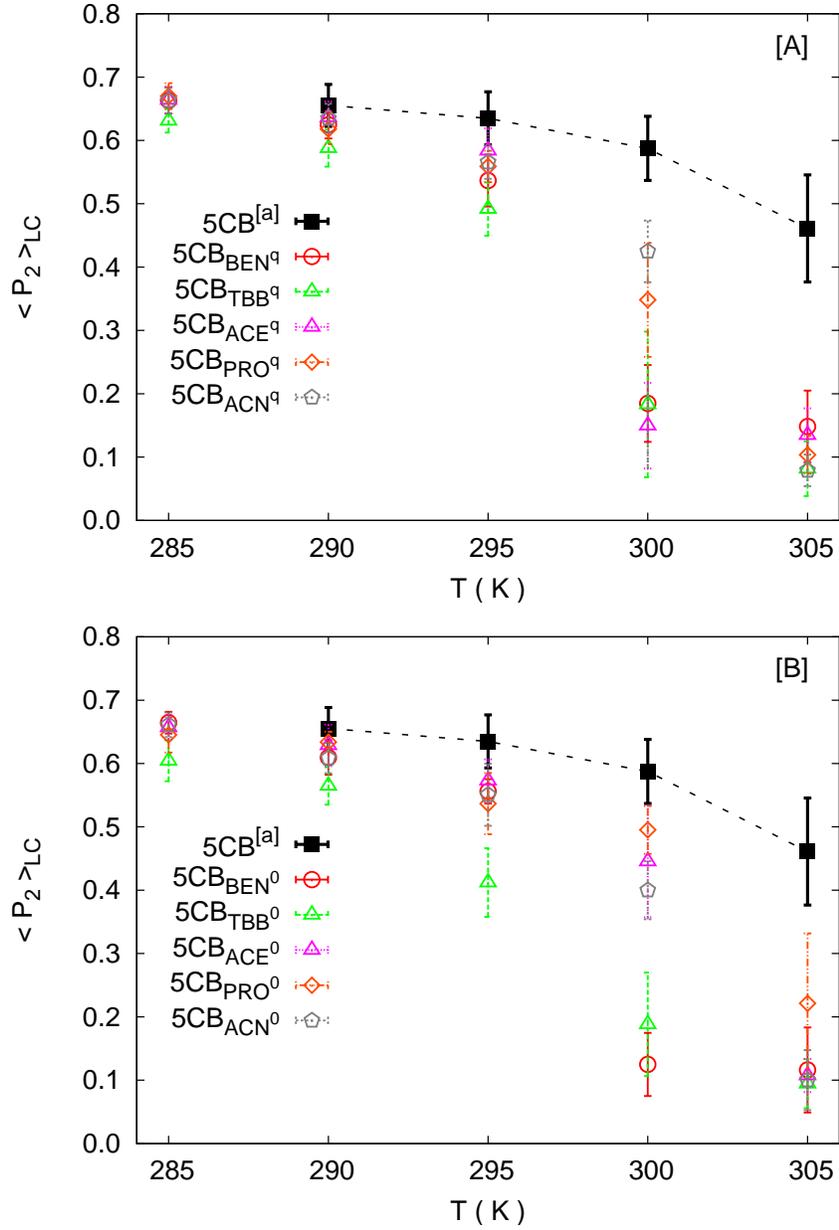
Figure 3: Orientational order parameter $\langle P_2 \rangle_{LC}$ for the 5CB solvent from the MD simulations of various solutions with concentration $x = 0.04$ of standard solutes (A) and chargeless solutes (B) as a function of temperature T. The black squares [a] are the simulated order parameters for the pure solvent from ref.[22]
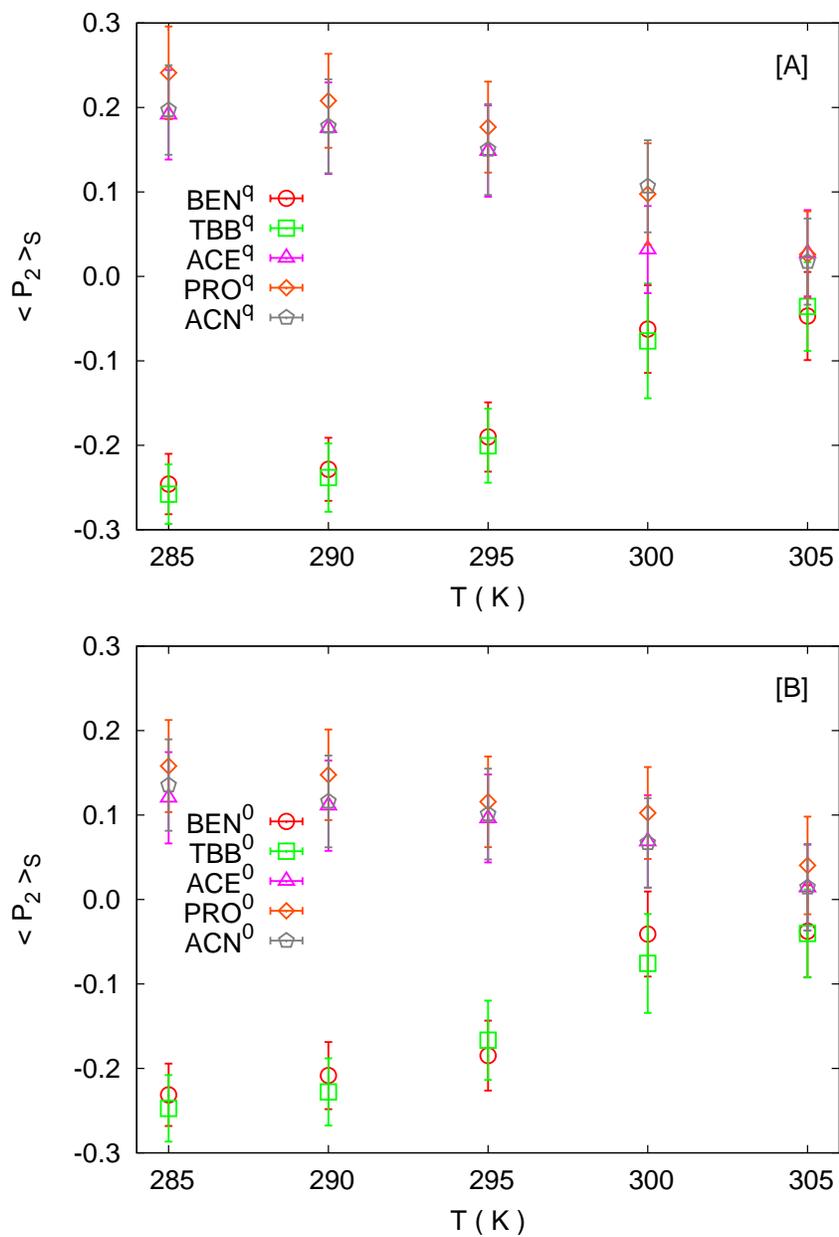
Figure 4: Average order parameter $\langle P_2 \rangle_S$ for standard (A) and chargeless solutes (B) as a function of temperature.
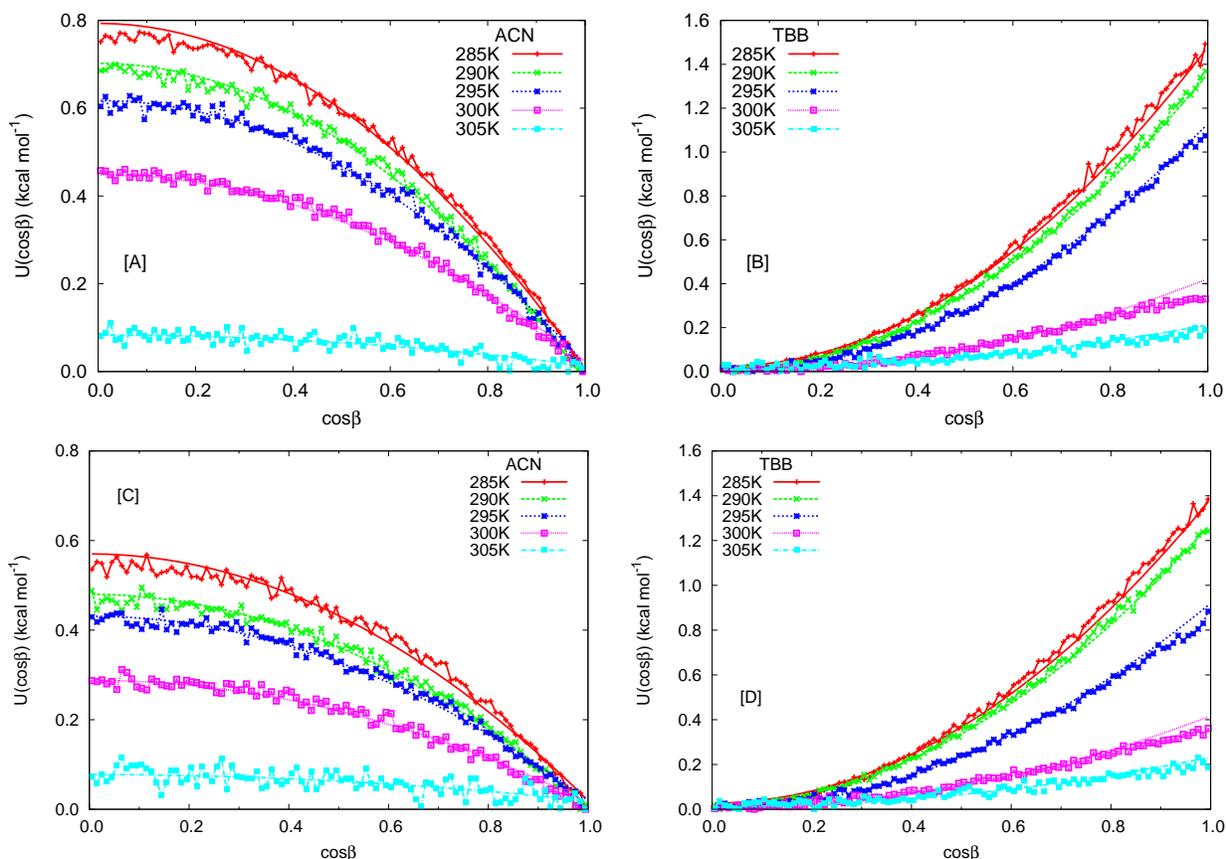
Figure 5: The effective orientational energies U($\cos\beta$) calculated from MD simulations and the respective effective potential fits (continuous lines) of a prolate (ACN) and an oblate (TBB) molecule at various temperatures. The results for standard ACN and TBB are shown in plates A and B while those for the chargeless solutes are shown in C and D.
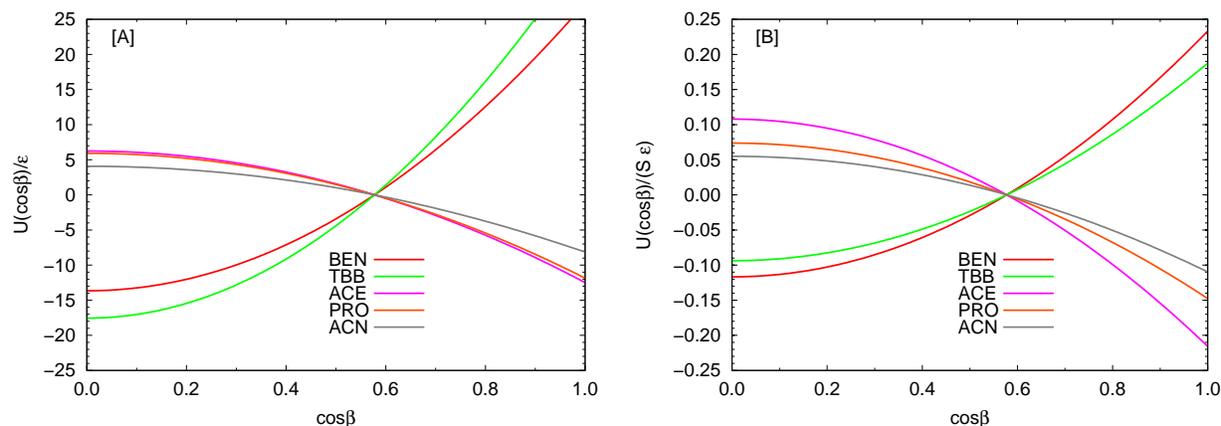

Figure 6: The orienting surface potential $U_{\text{ST}}/\varepsilon$ from 10 versus molecular orientation β (plate A), and the same function normalized by the molecular surfaces of Table 8 (plate B).
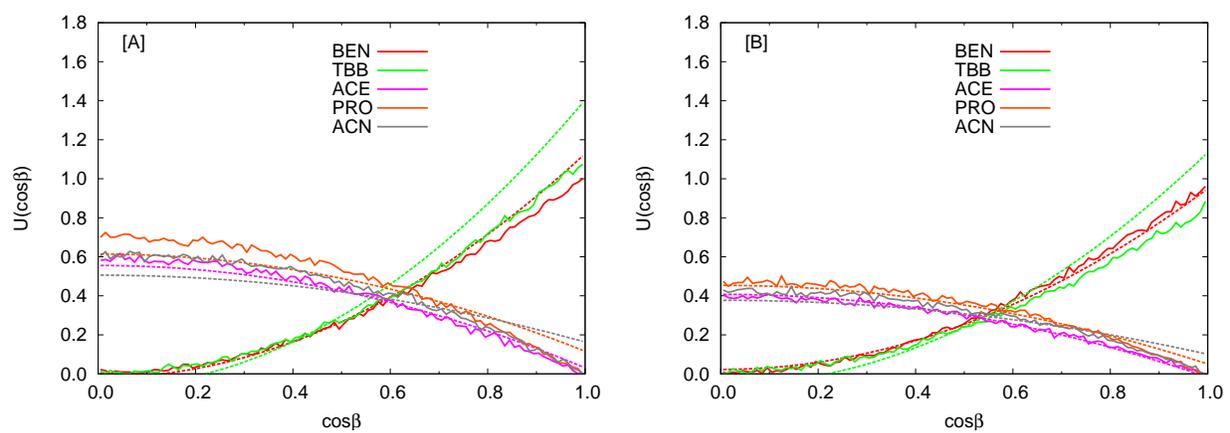
Figure 7: Orientational energies versus molecular orientation from the MD simulations at $T = 295$ K and the corresponding ones obtained from surface tensor model tensor fit (9) for standard (plate A) and chargeless (plate B) solutes.
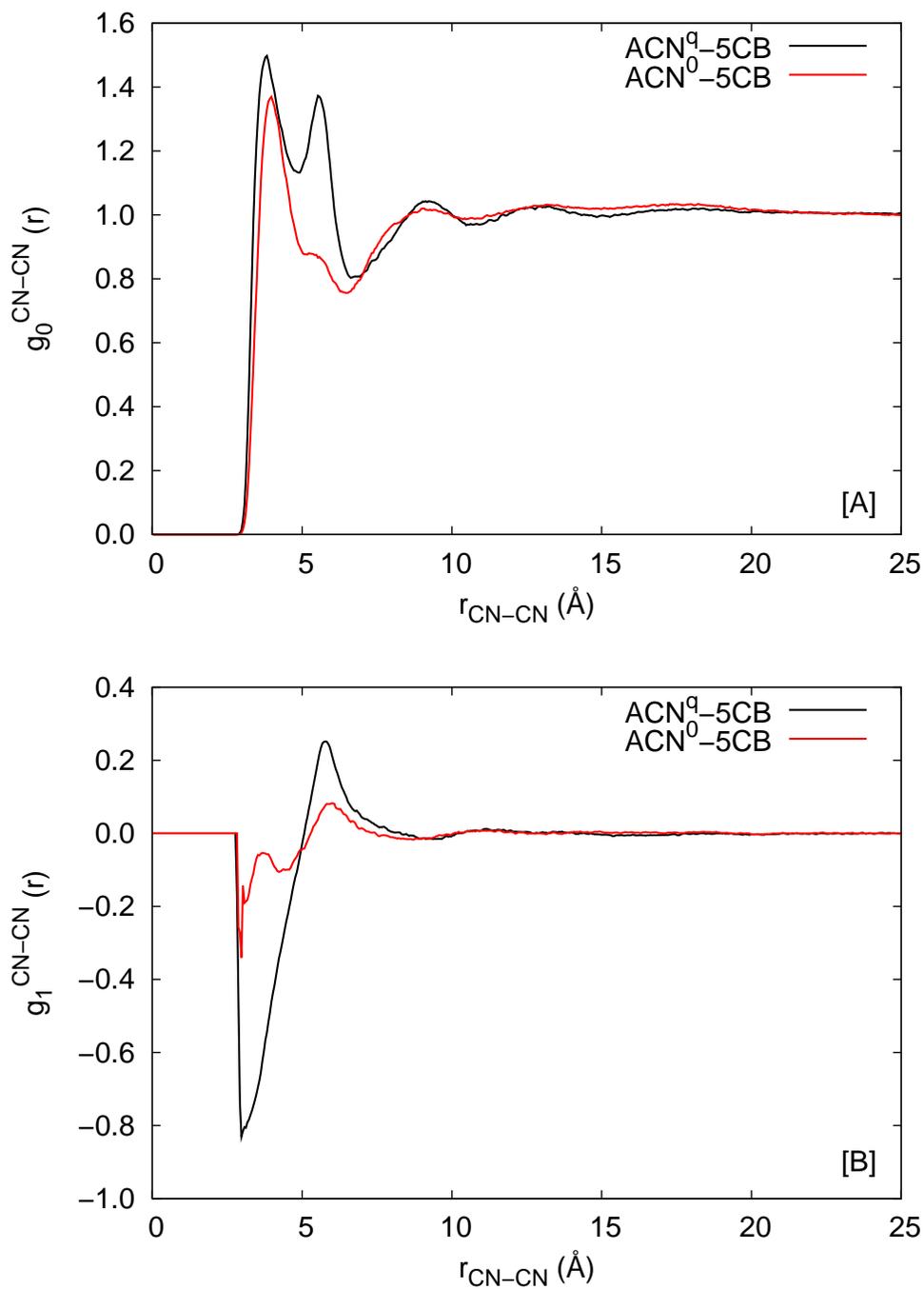
Figure 8: Radial, $g_0^{CN-CN}(r)$ (plate A), and polar, $g_1^{CN-CN}(r)$ (plate B), pair correlations calculated at $T = 285$ K between the cyano group of acetonitrile and the 5CB solvent as function of the distance between the midpoint of the CN bonds.